MODELS OF MASSIVE STARS IN HOMOLOGOUS GRAVITATIONAL CONTRACTION

By S. M. A. Meggitt*

[*Manuscript received February* 15, 1965]

Summary

Nine models of homologously contracting, uniform composition stars have been constructed for $\mu^2 M/M_\odot$ in the range 10–80. Apart from the two smallest models, all models have convective cores, the size of core increasing with the mass. The rate of contraction increases with mass up to $\mu^2 M/M_\odot = 32$ and decreases thereafter. One set of models covers all compositions.

I. Introduction

Previous investigations of the contraction of massive stars have been undertaken by Boury (1963) and by Van der Borght (1964). In these investigations it was assumed that contraction was homologous, and the relative distributions of the physical quantities were taken to be the same as in the corresponding main sequence model. This implies that there is no energy generated in the envelope and is a good approximation when there is a large convective core containing most of the mass. This can be expected to be the case for very massive stars, owing to the importance of the radiation pressure. On the other hand smaller stars are wholly radiative in the period immediately preceding nuclear burning.

Models are constructed here in which the energy generation in the radiative region is taken into account. It is shown that the equations of quasi-static equilibrium can be solved directly, independently of the radius, if it is assumed that (i) contraction is homologous, (ii) the energy source is entirely gravitational, (iii) the opacity is due to electron scattering, and (iv) the composition is uniform throughout the model. This leads to models which change from purely radiative at the lower masses to mainly convective at the higher masses. By extending the transformations used in Van der Borght and Meggitt (1963) to the energy equation, a one-parameter set of models suffices for all compositions. These models can be expected to be a good approximation to the structure of a massive star during the time when the surface temperature is high enough to ensure a radiative envelope, but before nuclear energy provides an appreciable proportion of the luminosity.

II. Equations

The assumptions of uniform composition and of electron scattering opacity imply that μ and κ are constant throughout the model. Also, in the absence of nuclear processes they do not change with time. In the basic differential equations for the stellar interior (Schwarzschild 1958, whose notation is used here), the composition and radius are removed from all equations except the energy equations

* Department of Mathematics, School of General Studies, Australian National University, Canberra.

((2), (5) below), by the substitutions $m = \mu^2 M_r$, $l = \kappa\mu^2 L_r$, $t = \mu RT$, following the procedure of Van der Borght and Meggitt (1963). Using the equation of state to eliminate the density and pressure, the differential equations become

$$\frac{\mathrm{d}m}{\mathrm{d}x} = \frac{4\pi a}{3\mathscr{R}}\cdot\frac{\beta t^3}{1-\beta}\cdot x^2, \tag{1}$$

$$\frac{\mathrm{d}l}{\mathrm{d}m} = \kappa\epsilon; \tag{2}$$

Convective

$$\left.\begin{aligned}\frac{\mathrm{d}t}{\mathrm{d}x} &= -\frac{G}{\mathscr{R}}\cdot\frac{\beta(8-6\beta)}{32-24\beta-3\beta^2}\cdot\frac{m}{x^2},\\ \frac{\mathrm{d}\beta}{\mathrm{d}x} &= \frac{G}{\mathscr{R}}\cdot\frac{3\beta^3(1-\beta)}{32-24\beta-3\beta^2}\cdot\frac{m}{x^2 t};\end{aligned}\right\} \tag{3}$$

Radiative

$$\left.\begin{aligned}\frac{\mathrm{d}t}{\mathrm{d}x} &= -\frac{1}{16\pi c\mathscr{R}}\cdot\frac{\beta}{1-\beta}\cdot\frac{l}{x^2},\\ \frac{\mathrm{d}\beta}{\mathrm{d}x} &= \frac{1}{4\pi c\mathscr{R}}\cdot\frac{\beta}{x^2 t}\{l-4\pi cGm(1-\beta)\};\end{aligned}\right\} \tag{4}$$

together with the expression for the energy released by contraction,

$$\epsilon = \frac{3\mathscr{R}T}{2\mu}\frac{\partial}{\partial\tau}(\ln T - 8y/3 - \tfrac{2}{3}\ln y), \tag{5}$$

where $y = (1-\beta)/\beta$, β is the ratio of gas pressure to total pressure, and τ is the time.

To these equations are added the boundary conditions $m = 0$, $l = 0$ at the centre, and $t = 0$ at the surface. The additional condition necessary at the surface has been taken as

$$\frac{\kappa L}{4\pi cGM(1-\beta)} = 1. \tag{6}$$

This is an approximation to the more precise condition

$$\left(\frac{T}{T_e}\right)^4 = \frac{1}{2\{1-\kappa L/4\pi cGM(1-\beta)\}},$$

which holds in a radiative region near the surface, in which M_r and L_r are taken as constant and in which $\kappa PR^2/GM$ has the value $\frac{2}{3}$ when $T = T_e$ (effective temperature).

The composition (which enters only through κ and μ) and the radius are removed from the energy equations (2) and (5) in the following way. The assumption of homologous contraction is that $q = M_r/M$ is independent of the time. By Lane's theorem (Chandrasekhar 1939) it follows that RT and β are independent of the time. Define the quantity K by

$$\frac{\mu^2}{\kappa K} = \frac{\mathrm{d}}{\mathrm{d}\tau}\left(\frac{1}{R}\right). \tag{7}$$

Equation (5) then becomes

$$\epsilon = 3\mathscr{R}t/2\kappa K. \tag{8}$$

The surface condition (6) shows that κL is constant during the contraction, that is,

$$\frac{3\mathscr{R}M}{2K}\int_0^1 t\,\mathrm{d}q = \text{constant}.$$

It follows that K is constant, and the contraction follows the usual pattern in which the reciprocal of the radius changes uniformly with time. Combination of (2) and (8) leads to the energy equation

$$\frac{\mathrm{d}l}{\mathrm{d}m} = \frac{3\mathscr{R}t}{2K}. \tag{9}$$

Equations (1), (3), (4), and (9) are now independent of both radius and time, and so may be integrated to give a model in a state of homologous contraction.

III. Method of Integration

The equations were integrated numerically on an IBM 1620 computer using the classical fourth-order Runge–Kutta method with a step length of 1% of the radius. Starting from the surface the values of two parameters, L and K, need to be chosen. The method described by Sears (1959) was used, in which the run of $U = \mathrm{d}(\ln M_r)/\mathrm{d}(\ln r)$ determines whether the initial choice of L is too large or too small. In a similar manner, a check on the value of K was obtained by observing the quantity $\mathrm{d}(\ln L_r)/\mathrm{d}(\ln M_r)$, which should increase monotonically from zero at the surface to unity at the centre. If this quantity decreases anywhere K is too large, and if it exceeds unity K is too small for the particular value of L chosen.

Each inward integration was terminated at $x = 0\cdot10$, and the central value β_c was estimated from the convective expansion

$$y = y_c - \frac{x^2}{2}\left(\frac{4\pi G\mu\rho R^2}{\mathscr{R}T}\cdot\frac{y}{5+40y+32y^2}\right)_c + \frac{x^4}{24}\left(\frac{16\pi^2G^2\mu^2\rho^2R^4y}{5\mathscr{R}^2T^2}\cdot\frac{70+120y+768y^2+1024y^3}{(5+40y+32y^2)^3}\right)_c,$$

while T_c was obtained from constancy of the entropy

$$(\tfrac{2}{3}\ln y + 8y/3 - \ln T)(3\mathscr{R}/2\mu)$$

in the core. These values were used to start an integration from the centre out to the point $x = 0\cdot10$. The differences between the values of β and T at this point from the inward and outward integrations were used to improve the estimates of T_c and β_c, and the differences in M_r and L_r were used to improve the values of the parameters L and K. So long as these differences were less than 1% of the quantities involved, linear extrapolation in two variables gave excellent results.

IV. Results

The results of the integrations are set out in Table 1. With the exception of the models $\mu^2M/M_\odot = 10$ and $12 \cdot 5$, which are purely radiative, all models were found to have convective cores and radiative envelopes. Interpolation in the Schwarzschild condition shows that convection appears at the centre when $\mu^2M/M_\odot = 13 \cdot 1$. The subscripts c, f, s refer to the centre, boundary between core and envelope, and surface respectively. The numbers in the row labelled P.E. are the coefficients of $-GM^2/R$ in the expression for the potential energy. Comparison with the value

$$-\frac{3}{5-n} \cdot \frac{GM^2}{R}$$

for a polytrope shows an average polytropic index varying between $2 \cdot 76$ and $2 \cdot 6$.

Table 1

RESULTS OF NUMERICAL INTEGRATIONS

$\mu^2M/M_\odot$	10	12·5	15	20	25	30	40	60	80
$10^{-5}K$	1·122	1·030	0·976	0·920	0·896	0·887	0·891	0·930	0·982
$\log_{10}(\kappa\mu^2L/L_\odot)$	4·204	4·407	4·563	4·793	4·962	5·094	5·294	5·558	5·735
$\mu RT_c/10^6R_\odot$	148	173	195	232	264	295	350	447	532
$\rho_c/\bar{\rho}$	31·6	29·7	28·1	26·2	25·3	24·9	24·9	25·6	26·5
x_f	—	—	0·147	0·262	0·327	0·372	0·433	0·504	0·546
q_f	—	—	0·076	0·302	0·458	0·564	0·695	0·818	0·874
L_f/L	—	—	0·122	0·429	0·607	0·713	0·827	0·916	0·949
β_c	0·818	0·769	0·727	0·662	0·614	0·576	0·519	0·444	0·395
β_f	—	—	0·740	0·697	0·662	0·631	0·582	0·509	0·458
β_s	0·879	0·845	0·815	0·765	0·722	0·686	0·627	0·544	0·486
P.E.	1·337	1·319	1·303	1·279	1·265	1·256	1·249	1·250	1·257

The constant K is defined by equation (7), and is tabulated so that κK is in units of (years) $\times$ (solar radii) if κ is expressed in cm^2/g. It gives a measure of the Helmholtz contraction time in the sense that if the model were to contract from an infinite radius, $\kappa K/\mu^2$ would be the time in years to contract to one solar radius. It can be seen that the rate of contraction reaches a maximum for $\mu^2M/M_\odot = 32$, more massive models contracting more slowly. In fact, for large masses K will increase in proportion to the square root of the mass. For, as M increases the model approaches a completely convective state in which radiation pressure is dominant. Under these circumstances Hoyle and Fowler (1963) have shown that a good approximation is obtained by using a polytrope of index 3. This satisfies the relation

$$0 \cdot 0031(\mu\beta)^4(M/M_\odot)^2 = 1-\beta, \tag{10}$$

and has potential energy $-3GM^2/2R$. Since only the proportion $\beta/2$ of the energy is available for radiation, we have

$$L = \frac{\beta}{2}\frac{d}{d\tau}\left(\frac{3GM^2}{2R}\right).$$

Substitution of K from (7), β from (10), and L from (6) with $1-\beta \approx 1$ leads to

$$K = 7 \cdot 7 \times 10^3 (\mu^2 M/M_\odot)^{\frac{1}{4}}.$$

The models for large masses differ little in relative distribution of β, q, and T from static homogeneous models. The only difference lies in the energy equation.

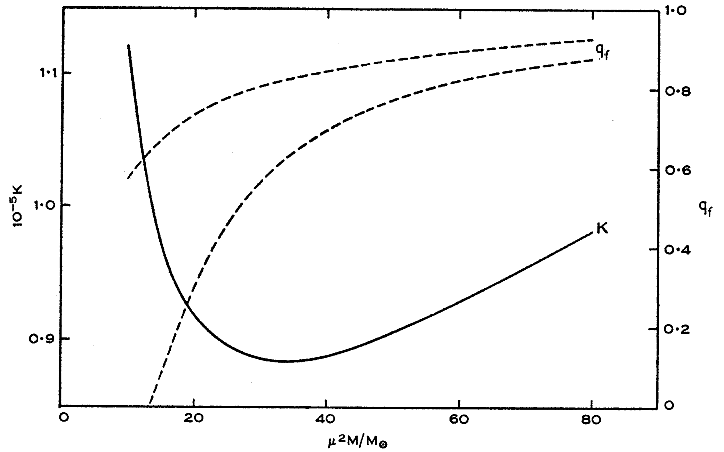

Fig. 1.—Variation of K and q_f with mass. Upper dashed curve: main sequence models (Van der Borght and Meggitt); lower dashed curve: models constructed in the present paper.

In the contracting models part of the energy is produced outside the core; in the static models all of the energy is produced in the core. As the size of the core increases with mass the difference between the two types of models diminishes (Fig. 1). Table 2

TABLE 2

COMPARISON BETWEEN CONTRACTING AND STATIC HOMOGENEOUS MODELS FOR $\mu^2 M/M_\odot = 80$

Characteristic	Contracting Model	Static Model
$\log_{10}(\kappa\mu^2 L/L_\odot)$	5·735	5·729
$\mu R T_c/10^6 R_\odot$	532	528
$\rho_c/\bar{\rho}$	26·5	25·6
x_f	0·546	0·608
q_f	0·874	0·924
L_f/L	0·949	1
β_c	0·395	0·393
β_f	0·458	0·469
β_s	0·486	0·492

compares the properties of the most massive contracting model considered here with those of the corresponding static homogeneous model. The effect of the 5% of the luminosity which is generated in the envelope of the contracting model is seen to be small.

V. Acknowledgment

It is a pleasure to express my appreciation to Professor R. Van der Borght for many valuable discussions.

VI. References

Boury, A. (1963).—*Mém. Soc. R. Sci. Liège* (5) **8**: Part 6.

Chandrasekhar, S. (1939).—"An Introduction to the Study of Stellar Structure." (Univ. of Chicago Press.)

Hoyle, F., and Fowler, W. A. (1963).—*Mon. Not. R. Astr. Soc.* **125**: 169.

Schwarzschild, M. (1958).—"Structure and Evolution of the Stars." (Princeton Univ. Press.)

Sears, R. L. (1959).—*Mém. Soc. R. Sci. Liège* (5) **3**: 479.

Van der Borght, R. (1964).—*Aust. J. Phys.* **17**: 165.

Van der Borght, R., and Meggitt, S. (1963).—*Aust. J. Phys.* **16**: 415.

POLARIZATION OF TYPE III BURSTS

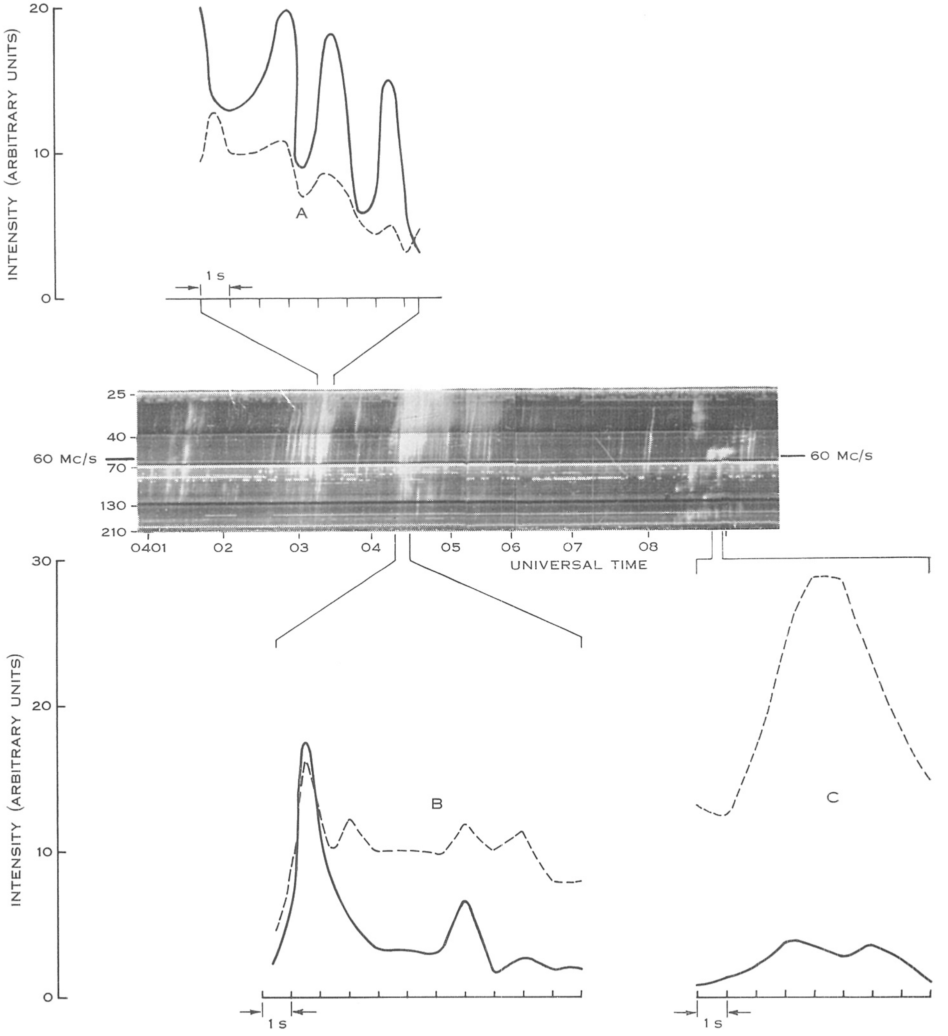

Variation of polarization with time during groups of type III bursts. The polarized component is shown by full lines, the unpolarized by dashed lines.